



DIGITAL
LIBRARY

dspace.vutbr.cz

Electrically reading a light-driven molecular switch on 2D-Ti₃C₂T_x MXene via molecular engineering: towards responsive MXetronics

MUÑOZ MARTIN, J.; PALACIOS CORELLA, M.; PUMERA, M.

Journal of Materials Chemistry A
2022, vol. 10, iss. 32, pp. 1701-1708

ISSN: 2050-7496

DOI: <https://doi.org/10.1039/d2ta03349f>

Accepted manuscript

Electrically Reading a Light-Driven Molecular Switch on 2D-Ti₃C₂T_x MXene *via* Molecular Engineering: Towards Responsive MXetronics

Jose Muñoz,^a Mario Palacios-Corella,^a Martin Pumera^{a,b,c,d,*}

^a Future Energy and Innovation Laboratory, Central European Institute of Technology, Brno University of Technology, Purkyňova 123, 61200 Brno, Czech Republic

^b Energy Research Institute@NTU (ERI@N), Research Techno Plaza, X-Frontier Block, Level 5, 50 Nanyang Drive, 637553 Singapore, Singapore

^c Department of Medical Research, China Medical University Hospital, China Medical University, No. 91 Hsueh-Shih Road, Taichung, 40402 Taiwan

^d Department of Chemical and Biomolecular Engineering, Yonsei University, 50 Yonsei-ro, Seodaemun-gu, Seoul 03722, Korea

* Corresponding author: martin.pumera@ceitec.vutbr.cz

Abstract

The contemporary digital revolution, which demands for miniaturized electronics, has prompted the search for molecule-based nanomaterials that handle some of the computational logic functions—which relates the concept of zeros (0) and ones (1) in binary code—reached by mainstream silicon-based semiconductor technology. Herein, the feasibility of emerging 2D transition metal carbide (MXene) derivatives to write, erase and readout bistable molecular switches has been elucidated. As a first demonstration of applicability, 2D-Ti₃C₂T_x MXene has been covalently functionalized with an optically active molecule as azobenzene (AZO), in which the photo-driven inputs of the AZO isomerization ($E\text{-AZO@Ti}_3\text{C}_2\text{T}_x \leftrightarrow Z\text{-AZO@Ti}_3\text{C}_2\text{T}_x$) resulted in two distinguished electrical states when it was immobilized in an emerging 3D-printed transducer. Thus, this work provides the basis towards the yet undisclosed concept of “*Responsive MXetronics*” by molecularly engineering smart MXenes to perform logic (opto)electronic tasks.

Keywords: 2D materials; Azobenzene; 3D-printed electrodes; Optoelectronics; Logic gates

1. Introduction

The ability of electronic devices to act as switches makes digital information processing possible. The development of electronic devices can be described using Moore's Law, which postulates that computing power doubles roughly every year and a half.^{1,2} To date, conventional silicon-based semiconductor processors, which are fabricated according to a top-down principle, have been at the forefront of this technology.^{3,4} However, the increasing demand on miniaturizing electronic devices, together with the challenging production of silicon-based electronics at the nanometer scale,^{5,6} has prompted the search for molecule-based digital processing and communication (Molecular Electronics).⁷⁻⁹ In this regard, molecular engineering is currently leading the global "Fourth Industrial Revolution" —also called as Industry 4.0, described as the convergence of digital technologies with breakthroughs in Materials Science, Chemistry and Biology to progress in the deep digital transformation— through the use of molecular-level science to supply "intelligent" materials and devices with entirely new and advanced capabilities for people and machines.^{10,11} Molecular Electronics can be seen as computational processors of physical or chemical inputs to generate a single output following a set of logical operations, which relates to the concept of logical zeros (0) and ones (1) in binary code.¹² The translation of an external input (*i.e.*, chemical, optical, electrical, etc.) into a readable output signal can be achieved using responsive materials, which result from the confinement of active molecular components upon passive materials to promote bistable switches.^[11] Bistability relies on the existence of two or more thermodynamically stable states in a single system, making possible to apply binary logic (0, 1). Ferrocene,

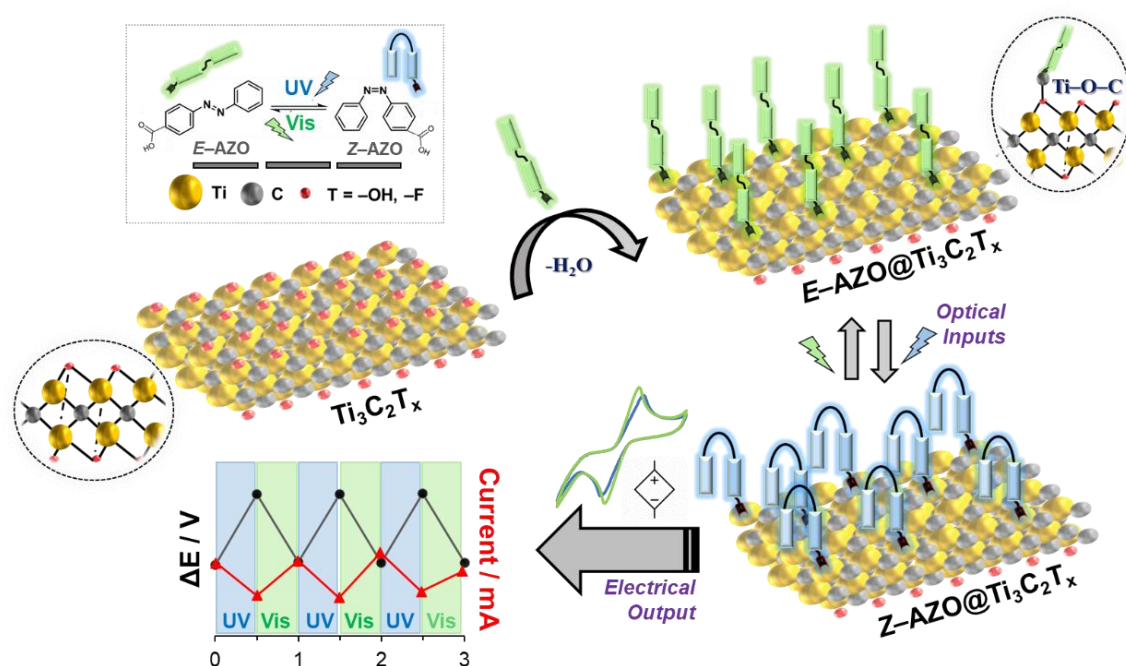
azobenzene, imidazole or cyclodextrin represent prominent examples of (supra)molecular components that display bistable active forms in solution when they are subjected to an external trigger (*e.g.*, electrical, optical, chemical or supramolecular, respectively).^[12] In particular, the readout of electrical signals between two well-defined bistable molecular states has been at the heart of the modern information due to the accessible miniaturization of electronic components.^{15–17} Thus, engineering responsive conductive nanomaterials harboring stimuli-responsive molecules represent an efficient pathway to electrically monitoring bistable molecular switches.^{18–20} Although extremely motivating from a scientific point of view, retaining the bistability of molecules on the surface of interest is a chemical challenge.

MXenes —referring to a new class of 2D layered transition metal carbide structures beyond mainstream graphene— have recently aroused extensive attention in the materials science community for a wide range of applications.^{21–24} MXenes have a general formula of $M_{n+1}X_nT_x$ —where M stands of an early transition metal (*e.g.*, Ti, Mo, V or Cr), X represents C and/or N elements, and T_x symbolizes the surface-terminating functionality (*e.g.*, –O, –OH and –F) with n ranging from 1 to 3—, being titanium carbide (2D-Ti₃C₂T_x) the most widely studied, and therefore representative metallic MXene member.^{25,26} In particular, 2D-Ti₃C₂T_x presents unique characteristics, such as high surface area, good chemical stability and tunable surface functionality, that in combination with its inherent metallic conductivity and hydrophilic TiO₂-like surface, endow it with outstanding electrochemical performances for MXetronics (which allude to electronic and photonic applications of MXene-based devices).^{27,28} Nonetheless, since this research is still in an early stage, the main bottleneck in the field of MXetronics relies on the limited library of responsive MXenes acting as switches for molecular logic gates development.²⁹ This drawback could be overcome by the confinement of *ad hoc* active

molecular components on MXenes in order to translate a molecular signal into a readable macroscopic change. In this regard, the assembly of organic molecules has resulted in a simple and effective synthetic methodology to tailor the physicochemical properties according to task-specific applications. The presence of reactive terminal groups (T_x) renders the MXene surfaces suitable to accommodate different architectures *via* a bottom-up assembly strategy, making possible to tune the properties of MXenes.³⁰⁻³⁴ Such a tunability with active molecules would enable further possibilities to cover the current gap in the field of MXetronics due to the acquisition of programmable properties.

Herein, motivated by the possibility to advance in the field of MXetronics, a straightforward and sustainable strategy has been devised to produce Responsive MXenes capable of writing, reading and erasing bistable molecular switches *via* implanting active molecular moieties. As a first demonstration of applicability, 2D- $Ti_3C_2T_x$ has been covalently functionalized with an optically active molecule as azobenzene (AZO) by esterification chemistry, since it entails a prominent example of photo-responsive molecule in which the conformational changes, as a result of a reversible *E/Z* isomerization upon irradiation, form the basis of a light-driven bistable molecular switch (see **Scheme 1** for illustration).^{35,36} To date, several photo-responsive carbon nanomaterials (e.g., graphene, carbon nanotubes or fullerenes) have been achieved by grafting AZO moieties.³⁷ Further, a recent work has reported the functionalization of 2D- $Ti_3C_2T_x$ with an AZO derivative *via* weak electrostatic interactions³⁸ (rather than the covalent esterification reaction report here). However, it is important to point out that no photo-switchable studies were considered. To achieve this, the electrical output signals of the resulting AZO@ $Ti_3C_2T_x$ were modulated (write/erase) with external light stimuli and electrochemically monitored (readout) by means of cyclic voltammetry (CV), using an emerging 3D-printed nanocomposite carbon electrode (3D-nCE) as a model

transducing platform to reach a proof MXetronic prototype.^{39,40} In this regard, 3D printing has proven to be a powerful technology for the large-scale manufacture of free-form electronic devices on-demand.^{41,42} Interestingly, two electrical states (0, 1) at the MXetronic/electrolyte interface were successfully discerned by CV. Accordingly, the significant findings of this proof-of-concept paves the way towards the yet undisclosed concept of “*Responsive MXetronics*” by devising programamable MXenes carrying active molecules, which supposes the principle to reach complex logic functions at the molecular level on-demand. In light of the state-of-the-art, the combination of molecular engineering and 2D-Ti₃C₂T_x foresees a promising pathway towards the development of a new family of Molecular MXetronics to extend their implementation in alternative fields, such as switching memories, logic gates and (bio)sensors.



Scheme 1. Schematic illustration of the approach. Covalently functionalization of 2D-Ti₃C₂T_x with AZO molecules *via* esterification chemistry to achieve a photo-responsive AZO@Ti₃C₂T_x, in which the switchable optical inputs of the AZO isomerization ($E\text{-AZO@Ti}_3\text{C}_2\text{T}_x \leftrightarrow Z\text{-AZO@Ti}_3\text{C}_2\text{T}_x$) have been electrically discerned *via* cyclic voltammetry (output signals). Insets: structures of pristine and functionalized 2D-Ti₃C₂T_x.

2. Experimental Section

2.1. Materials and reagents

2D-Ti₃C₂T_x was purchased from Laizhou Kai Kai Ceramic Materials Co., Ltd. (Hong Kong S.A.R). 4-(phenylazo)benzoic acid (AZO), phosphate-buffered saline (PBS) electrolyte and tetrafluoroethylene-perfluoro-3,6-dioxa-4-methyl-7-octenesulfonic acid copolymer (Nafion 117 containing solution, ~5% in a mixture of lower aliphatic alcohols and water) and sulfuric acid (96% wt.) were obtained from Sigma-Aldrich (Germany). A commercially available conductive graphene/poly(lactic acid) filament (BlackMagic, Graphene Supermarket, USA) was employed for 3D-nCE fabrication. Organic solvents (dimethyl sulfoxide (DMSO) and isopropyl alcohol (IPA)) were of HPLC grade and supplied by Penta s.r.o. (Czech Republic).

2.2. Synthesis of photo-responsive AZO@Ti₃C₂T_x

Firstly, 2D-Ti₃C₂T_x was sonicated in deionized water and sonicated for 30 min in an ultrasonic homogenizer probe (amplitude 70%, 29 s of sonication and 20 s of resting). Afterwards, 10 mg of 2D-Ti₃C₂T_x and 10 mg of AZO were mixed in 1 mL DMSO containing 100 µL H₂SO₄ (96% wt.) and aged overnight at 60 °C under stirring conditions to induce the esterification chemistry. Finally, the resulting photo-responsive AZO@Ti₃C₂T_x was collected by centrifugation, washed several times with DMSO and IPA and dried to the air. The AZO@Ti₃C₂T_x material was stored in powder form, while fresh aqueous dispersions were prepared for the measurements in order to prevent its oxidation with water over time.

2.3. Apparatus and procedures

Material characterization of AZO@Ti₃C₂T_x was carried out by means of scanning electron microscopy coupled to an energy-dispersive X-ray spectroscopy detector (SEM-EDX, Tescan LYRA3) for morphological characterization and elemental mapping

composition, X-ray photoelectron spectroscopy (XPS, Kratos AXIS Supra) to analyze the atomic composition at the surface level, Fourier-transform infrared spectroscopy (FTIR, Bruker Vertex 80v) and ultraviolet-visible spectroscopy (UV-Vis, JASCO V-730) to identify functional groups, and thermogravimetric analysis (TGA, TA Instrument) under N₂ atmosphere (ramp: 10 °C·min⁻¹ up to 700 °C) to quantify the organic content. Studies of wettability were run by water contact angle (SEE-SYSTEM) employing 3 μL of deionized water. For this, samples were prepared by collecting 3 mL of AZO@Ti₃C₂T_x (concentration: 1 mg·mL⁻¹, solvent: IPA) in a cyclopore track etched membrane (pore size: 0.4 μm) using a vacuum pump. For comparison purpose, same experiments were conducted employing the pristine 2D-Ti₃C₂T_x material.

2.4. Electrochemical redout of the light-driven molecular switch

Electrochemical experiments were run in an Autolab PGSTAT204 potentiostat (Metrohm, Switzerland). For electrically monitoring the molecular switch, 120 μL of a fresh aqueous dispersion of AZO@Ti₃C₂T_x (5 mg·mL⁻¹) was drop-casted upon a 3D-nCE surface and used as a model transducing system, which was fabricated as previously reported (see **Figure S1** for illustration).^{43,44} The AZO@Ti₃C₂T_x dispersion was prepared in 3:2 IPA/H₂O containing 2% (v/v) of Nafion. The two different states (*E*-AZO@Ti₃C₂T_x ↔ *Z*-AZO@Ti₃C₂T_x) were photo-driven by irradiating the working electrode with an external light source (λ_{UV} : 365 nm; λ_{vis} : 465 nm) for 15 min and electrochemically read out by means of CV employing a three-electrode configuration cell filled with 0.1 M PBS as the electrolyte (scan rate: 50 mV·s⁻¹). A Pt wire, an Ag/AgCl and the drop-casted 3D-nCE (MXetronic) were used as the counter, reference and working electrodes, respectively. The reversibility of the molecular switch was considered doing 3 different cycles.

3. Results and Discussion

3.1. Characterization of photo-responsive AZO@Ti₃C₂T_x

Differently to a previous report in which 2D-Ti₃C₂T_x was decorated with an AZO derivative *via* weakly ionic interactions,³⁸ herein a covalently functionalized AZO@Ti₃C₂T_x was realized *via* Ti–O–C bond formation. The driving force of the esterification chemistry relies on the dehydration reaction derived from the nucleophilic substitution between the terminal –OH sites and the carboxylic acid group from the AZO derivative in acidic catalytic media.⁴⁵ The successful formation of the photo-responsive MXene (AZO@Ti₃C₂T_x) was confirmed employing a wide range of characterization techniques, including SEM, EDX, XPS and UV-vis spectroscopy (**Figure 1**). Additional characterization data by means of FTIR and TGA is also provided in Supporting Information (see **Figure S2-S3**).

The morphological characteristics of 2D-Ti₃C₂T_x before (control) and after being functionalized with AZO molecules were evaluated by SEM. As shown in **Figure 1a**, the pristine 2D-Ti₃C₂T_x exhibited the typical accordion-like structure.⁴⁶ After AZO anchoring, no significant morphological changes were noticed (**Figure 1b**), suggesting that the AZO molecules might be distributed mainly on the edge of the 2D-Ti₃C₂T_x walls rather than intercalated between the walls. The elemental mapping of AZO@Ti₃C₂T_x revealed a homogeneous distribution for C, Ti, O and N (**Figure 1c-g**). In particular, the apparition of N into the composition material together with its uniform distribution throughout the edges of the studied surface (**Figure 1g**) advocates the formation of the photo-responsive AZO@Ti₃C₂T_x. To further verify this, the surface chemical composition was also explored by XPS. **Figure 1h** depicts the XPS survey spectra of pristine 2D-Ti₃C₂T_x and functionalized AZO@Ti₃C₂T_x. While both materials exhibited three main contributions (attributed to Ti 2p, C 1s and O 1s), an additional peak around

400 eV was clearly observed after AZO functionalization, which must correspond to the N 1s signal of AZO molecules. Although the N 1s peak confirms the presence of the organic moiety in the functionalized MXene, the interacting nature between both components is not revealed. In order to reach a deeper and better understanding about such interaction, the high-resolution Ti 2p spectra of both pristine 2D-Ti₃C₂T_x and AZO@Ti₃C₂T_x were compared. **Table 1** summarizes the binding energy attributions for Ti 2p. As shown in **Figure 1i**, the Ti 2p spectrum of AZO@Ti₃C₂T_x not only displayed the main three chemical species for 2D-Ti₃C₂T_x (**Figure 1j**) but also an additional contribution fitted at 456.3 eV (Ti 2p_{3/2}) and 463.2 eV (Ti 2p_{1/2}). According to literature, these additional features can be assigned to the specific Ti–O–C bond formation, demonstrating the covalent nature of the molecular assembly.^{30,31} In concordance with XPS measurements, FTIR analysis also suggested the covalent functionalization by transferring the basic characteristic peaks from AZO to 2D-Ti₃C₂T_x, as well as the presence of a new peak at 886 cm⁻¹ in the FTIR spectra of AZO@Ti₃C₂T_x that has been previously associated to the Ti–O–C vibration (see **Figure S2**).⁴⁷ Therefore, the nature of the covalent assembling is consistent with both XPS and FTIR analyses.

By taking advantage of the optical properties of the molecular moiety (AZO), an additional UV-vis characterization was also considered to further support such results. The absorption wavelength of AZO depends on the particular molecular structure.⁴⁸ As shown in **Figure 1k**, the two main absorption bands associated to the raw AZO molecule⁴⁹—one in the ultraviolet region ($\lambda_{UV,max} = 327$ nm, high-intensity $\pi-\pi^*$ absorption) and another one in the visible region ($\lambda_{Vis,max} = 441$ nm, low-intensity $n-\pi^*$ absorption), see inset— were clearly blue-shifted to 278 nm ($\lambda_{UV,max}$) and 430 nm ($\lambda_{Vis,max}$) after being grafted to the MXene. This supposes an additional proof of the covalent nature of the anchoring. Finally, TGA analyses were run under N₂ atmosphere in order to quantify the

total amount of AZO grafted to 2D- $\text{Ti}_3\text{C}_2\text{T}_x$ (**Figure S3**). Comparing to pristine 2D- $\text{Ti}_3\text{C}_2\text{T}_x$, a total weight gain of 2.05% was yielded by the resulting $\text{AZO@Ti}_3\text{C}_2\text{T}_x$.

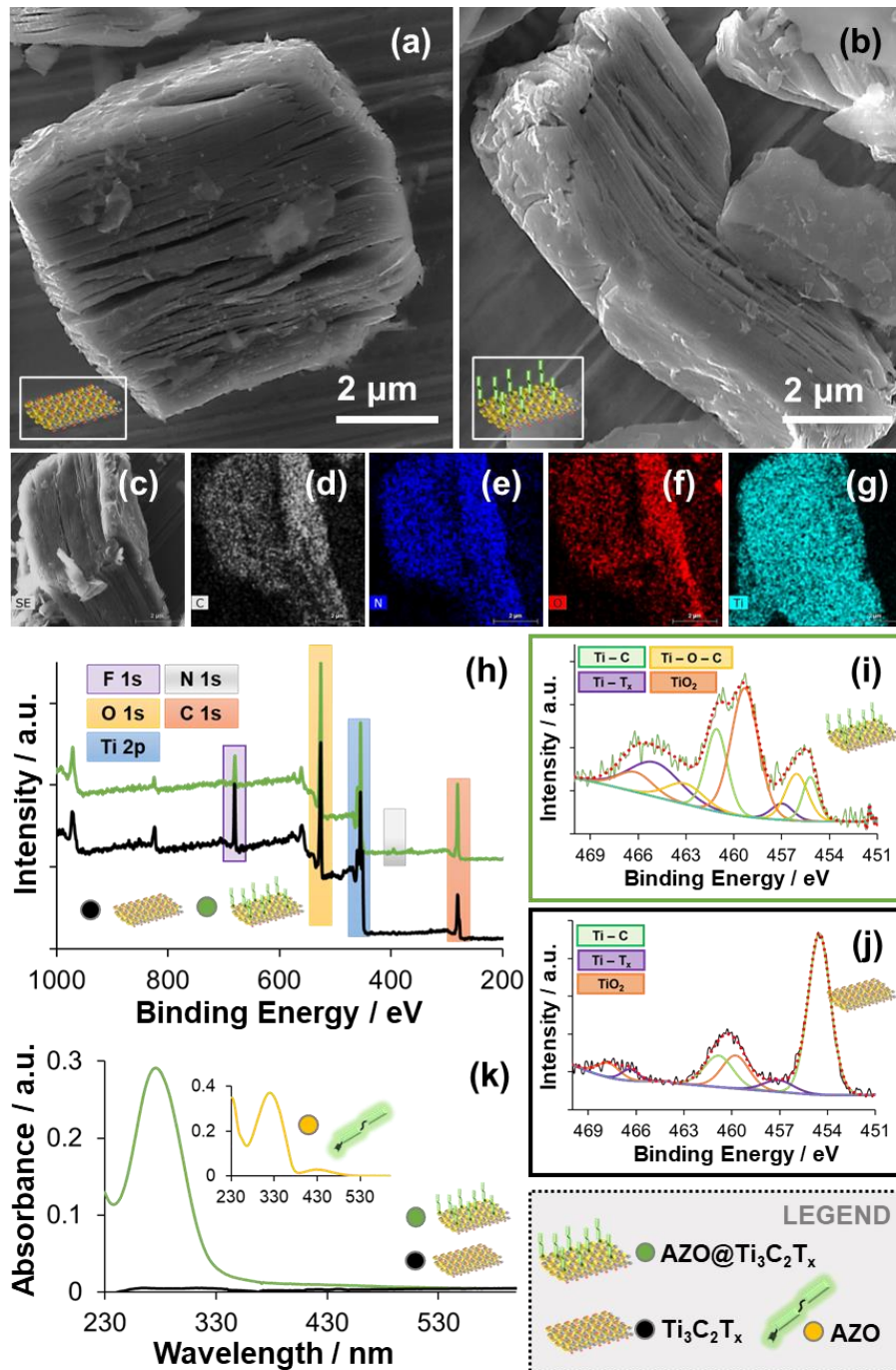










Figure 1. Material characterization of photo-responsive $\text{AZO@Ti}_3\text{C}_2\text{T}_x$. SEM images of (a) pristine $\text{Ti}_3\text{C}_2\text{T}_x$ and (b) $\text{AZO@Ti}_3\text{C}_2\text{T}_x$ with (c) its corresponding EDX elemental mapping for (d) C, (e) Ti, (f) O and (g) N. (h) XPS survey spectra of pristine $\text{Ti}_3\text{C}_2\text{T}_x$ and $\text{AZO@Ti}_3\text{C}_2\text{T}_x$, and (i-j) their corresponding high-resolution core level spectra of Ti 2p with the resulting contributions. (k) UV-vis spectra of pristine $\text{Ti}_3\text{C}_2\text{T}_x$, $\text{AZO@Ti}_3\text{C}_2\text{T}_x$ and raw AZO molecule (inset: blank experiment). Inset: legend of colors and material illustration.

According to all characterization data, it is safe to say that 2D-Ti₃C₂T_x was functionalized with AZO molecules *via* esterification chemistry, resulting in the photo-responsive AZO@Ti₃C₂T_x.

Table 1. Ti 2p binding energies (in eV) extracted from the corresponding high-resolution XPS spectra of pristine 2D-Ti₃C₂T_x and functionalized AZO@Ti₃C₂T_x.

Bond	TiO ₂ 2p _{1/2}	Ti-T _x 2p _{1/2}	Ti-O-C 2p _{1/2}	Ti-C 2p _{1/2}	TiO ₂ 2p _{3/2}	Ti-T _x 2p _{3/2}	Ti-O-C 2p _{3/2}	Ti-C 2p _{3/2}
2D-Ti ₃ C ₂ T _x	467.7	466.3	–	460.8	459.7	457.1	–	454.4
AZO@Ti ₃ C ₂ T _x	466.1	465.2	463.2	461.2	459.1	457.1	456.3	454.8
Color Legend								

3.2. Light-driven isomerization of photo-responsive AZO@Ti₃C₂T_x

AZO derivatives are stimuli-responsive molecules capable of undergoing a *trans/cis* (*E/Z*) isomeric transition *via* light irradiation. By applying a UV light source, the phenyl ring of *E*-AZO can be inverted, leading to the *Z*-AZO form. A reverse photo-isomerization from *Z*-AZO to *E*-AZO can be also reached by employing a visible light source. The geometrical changes resulting from such photoisomerization provides distinctive features (*i.e.*, different electric dipole moment and optical properties).^{50,51} Therefore, different photo-responsive performances of AZO@Ti₃C₂T_x before (*E*-AZO@Ti₃C₂T_x) and after UV irradiation (*Z*-AZO@Ti₃C₂T_x) were considered in order to elucidate whether the molecular characteristics of AZO isomers were successfully transferred to 2D-Ti₃C₂T_x (**Figure 2**).

On one hand, the optical properties of the photo-responsive AZO@Ti₃C₂T_x were studied by UV-Vis (**Figure 2a**). The absorption band centered at 430 nm—which corresponds to the *n*- π^* transitions of the *Z*-form—slightly increased after irradiation with UV light at 365 nm for 15 min, suggesting the isomerization from *E*-AZO@Ti₃C₂T_x

to Z -AZO@Ti₃C₂T_x.⁵² Subsequently, the photo-reversibility of the isomer formation was explored by exposing the sample to a 525 nm green light source for 15 min. As depicted in **Figure S4**, the n - π^* transition band decreased until yielding almost the beginning intensity due to the Z -to- E transformation, demonstrating the reversibility of the molecular switch.

On the other hand, the photo-triggered E -AZO@Ti₃C₂T_x to Z -AZO@Ti₃C₂T_x transition was also monitored by means of water contact angle (**Figure 2b-d**). The E -to- Z isomerization promotes changes on the electric dipole moment. While the straight form of E -AZO is almost non-polar (with a dipole moment close to 0 D), the polarity of the bent Z -form highly increases due to a dipole moment around 3 D.⁵³ Thus, a hydrophobic-to-hydrophilic transition of AZO@Ti₃C₂T_x is expected after UV irradiation. The water contact angle of pristine 2D-Ti₃C₂T_x, which was estimated to be lower than 5°, was considered as a control (**Figure 2b**). After grafting the AZO molecule to the MXene, the water contact angle of the resulting AZO@Ti₃C₂T_x remarkably increased up to $51.2 \pm 0.7^\circ$ due to the intrinsic hydrophobic skeleton of AZO molecules (**Figure 2c**). Upon UV irradiation, the contact angle of the AZO@Ti₃C₂T_x significantly diminished to $44 \pm 1^\circ$ due to the E -to- Z transition (**Figure 2d**), which supposes a decrease of 14%. Importantly, these results are also in agreement with the trend observed by zeta potential (ζ -potential, see **Figure S5**), since a higher absolute ζ -potential value was yielded by the Z -form (-29.9 ± 0.7 mV vs. the lower -20.6 ± 0.1 mV for E -form). Finally, the reversibility of the switch was further confirmed after irradiating the sample with a green light source, increasing the water contact angle value to $49.6 \pm 0.2^\circ$ (see **Figure S6**).

Thus, both optical and hydrophobic-to-hydrophilic transitions confirm that the molecular characteristics of AZO molecules were properly implanted onto the 2D-MXene, verifying the switchable nature of the photo-responsive AZO@Ti₃C₂T_x.

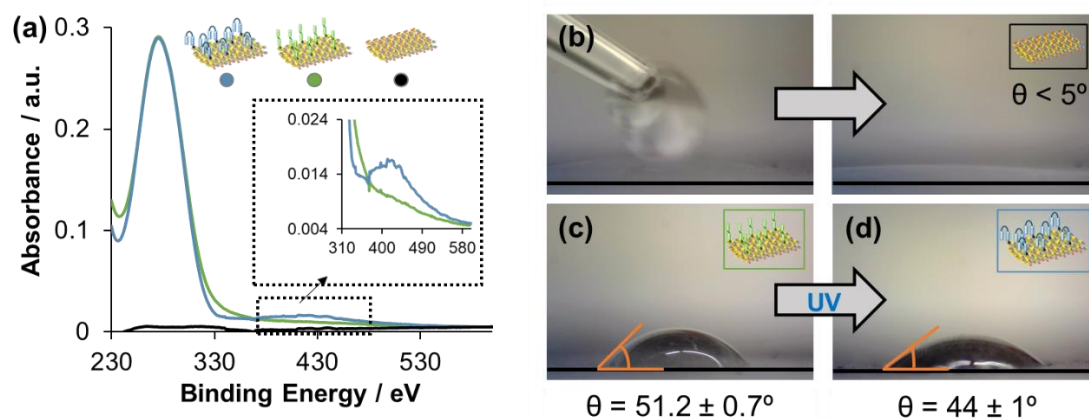


Figure 2. Photo-responsive performance of AZO@Ti₃C₂T_x before and after UV light irradiation. (a) UV-vis spectra of pristine Ti₃C₂T_x, and functionalized AZO@Ti₃C₂T_x before (*E*-AZO@Ti₃C₂T_x) and after UV irradiation (*Z*-AZO@Ti₃C₂T_x) using a material concentration of 0.12 mg·mL⁻¹. Water contact angle characteristics of (b) pristine Ti₃C₂T_x, (c) *E*-AZO@Ti₃C₂T_x and (d) *Z*-AZO@Ti₃C₂T_x (volume: 3 μL).

3.3. Electrical readout of a light-driven molecular switch for MXetronics

Having verified the transferred molecular properties of AZO to 2D-Ti₃C₂T_x, the last approach was focused on exploring the photoinduced isomerization ability of AZO@Ti₃C₂T_x to trigger (write) and reverse (erase) two different bistable molecular states (0, 1) in an electronic device. As a proof-of-principle, CV has been considered as the output system to read out the electrical interfacial changes derived from the two different bistable switches, using [Fe(CN)₆]^{3-/4-} as the benchmark redox marker. In this regard, electronic transduction tools are particularly appealing since electrical signals can be directly integrated with current nanotechnologies for developing novel logic elements for information processing. CV is an electrochemical tool that provides information regarding to the accessibility of the redox marker to be oxidized or reduced at the electrode surface. While the peak high intensity (*I_p*) is a parameter indirectly related to the interfacial charge transfer resistance at the electrode/electrolyte interface, the peak potential separation (*ΔE*) value determines the reversibility of the redox couple.⁵⁴ As a proof of MXetronic prototype, a proper amount of photo-responsive AZO@Ti₃C₂T_x was

drop-casted on an emerging 3D-nCE as a model transducing platform (see **Figure 3a** and Experimental Section for further details). The electrochemical measurements were run in a three-electrode configuration cell before and after *in situ* irradiating the MXetronic for 15 min with *i*) UV light at 350 nm (to obtain *Z*-AZO@Ti₃C₂T_x from *E*-AZO@Ti₃C₂T_x) and *ii*) visible light at 465 nm (to obtain *E*-AZO@Ti₃C₂T_x from *Z*-AZO@Ti₃C₂T_x).

Figure 3b reveals the CV performances of the MXetronic depending on the isomer nature of the photo-responsive AZO@Ti₃C₂T_x. Remarkably, the two light-triggered isomerization states (*E/Z* as the states 0 and 1, respectively) were dually discerned by means of ΔE ($\Delta_{\Delta E} = 0.15$ V) and I_p ($\Delta_{I_p} = 0.18$ mA). As illustrated in **Figure 3b** (inset), such voltammetric outcomes can be accounted by changes in the interfacial electron transfer reaction at the MXetronic/electrolyte interface promoted by the applied optical inputs. On one hand, the straight *E*-AZO@Ti₃C₂T_x form allows a tree-like molecular organization on the MXetronic surface that favors the formation of empty channels where the [Fe(CN)₆]^{3-/4-} redox marker can penetrate, fact that facilitates the interfacial electron transfer. From an electrochemical point of view, this can be translated as higher I_p (1.37 mA) and lower ΔE (0.50 V) values. Otherwise, the bent *Z*-AZO@Ti₃C₂T_x counterpart obtained after irradiation with UV light sterically hindered the MXetronic surface, blocking the interfacial electron transfer reaction that leads to lower I_p (1.19 mA) and higher ΔE (0.66 V) values. As shown in **Figure S7**, a control experiment carried out with pristine 2D-Ti₃C₂T_x did not display significant voltammetric changes before and after UV light irradiation, demonstrating the key role of the photo-switchable AZO molecule in the 2D-MXene. Finally, the reversibility of the photo-driven molecular switch was demonstrated by simply manipulating the external light source (from UV light at 365 nm to Vis light at 465 nm) for several cycles (**Figure 3c**).

Such promising results achieved at this optical input/electrical output system elucidate the suitability of MXene-based (opto)electronics carrying active molecules — herein referring to the term “*Responsive MXetronics*” — to discern electrical signals at the molecular level by combining active molecular components with 2D-Ti₃C₂T_x for binary logic (0, 1) processing.

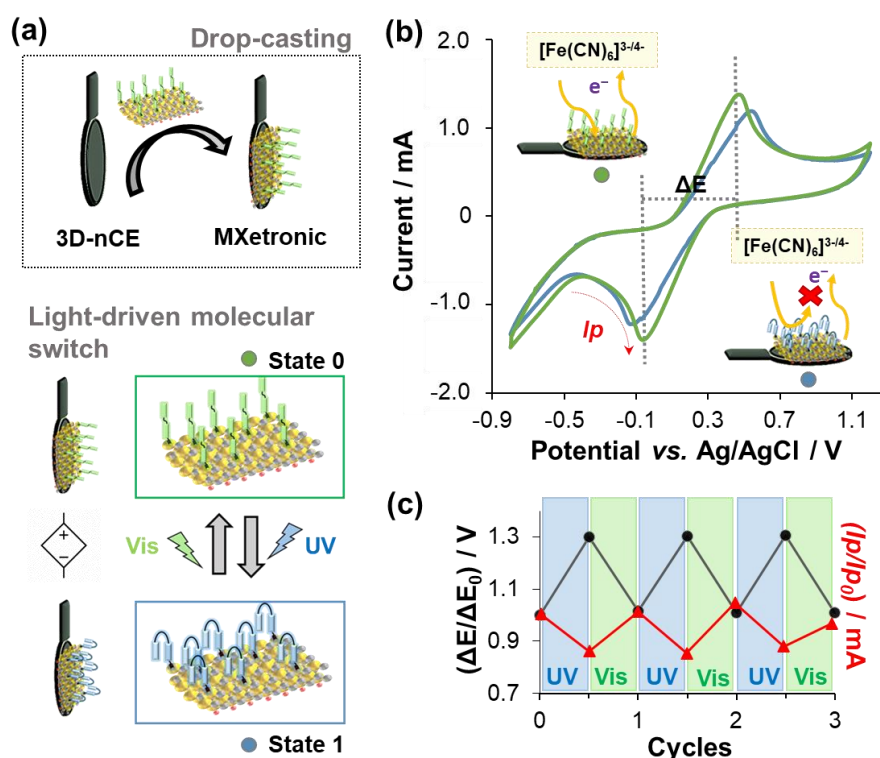


Figure 3. Electrically reading a bistable molecular switch at the photo-responsive AZO@Ti₃C₂T_x. (a) Illustration showing the immobilization of the photo-responsive AZO@Ti₃C₂T_x on the top of a 3D-printed nanocomposite carbon electrode (3D-nCE) to electrochemically discern two different light-driven states ($E\text{-AZO@Ti}_3\text{C}_2\text{T}_x \leftrightarrow Z\text{-AZO@Ti}_3\text{C}_2\text{T}_x$) at the MXetronic. (b) Electrochemical output signals obtained by CV (scan rate: 50 mV·s⁻¹) at the switchable MXetronic interface, using [Fe(CN)₆]^{3-/4-} as the benchmark redox marker. Inset: Illustration of the ability of the two different interfaces to properly oxidize/reduce the redox marker. (c) Dual electrochemical reversibility of the photo-switchable MXetronic achieved by CV in terms of ΔE and I_p .

4. Conclusions

A light-responsive MXene has been devised by covalently functionalizing 2D-Ti₃C₂T_x with a photo-active molecule as AZO *via* Ti–O–C bond formation. The inherent switchable molecular characteristics of AZO has shown to be successfully transferred to 2D-Ti₃C₂T_x, resulting in a photo-switchable AZO@Ti₃C₂T_x in which two bistable molecular states ($E\text{-AZO@Ti}_3\text{C}_2\text{T}_x \leftrightarrow Z\text{-AZO@Ti}_3\text{C}_2\text{T}_x$) have been successfully written and erased by manipulating the external light source. As a first demonstration of applicability, this AZO@Ti₃C₂T_x has been casted upon a 3D-printed transducer to achieve an MXetronic prototype to electrically read out a reversible light-triggered molecular switch *via* CV. As a result, a dual modulation of the electrochemical output signals was reached by means of current intensity peak (I_p) and peak potential separation (ΔE). Nonetheless, this supposes a proof-of-principle and therefore, some setup modifications should be considered for real implementation (*e.g.*, by fully 3D printing responsive MXetronics—rather than casting the material to the electrode to avoid some possible leakage—for *in situ* measurements in an integrated photoelectrochemical cell).

Overall, tuning 2D-Ti₃C₂T_x with active molecules has demonstrated to be a suitable approach to manipulate/control the electronic properties of MXenes. It is important to point out that the bottom-up functionalization approach is straightforward and might be simply customized through anchoring the desired active molecular moiety. Accordingly, this work represents an alternative to overcome the current bottleneck in the real applicability of 2D-MXenes by providing a new family of “*Responsive MXetronics*” which offer binary logic processing capabilities at the molecular level. Finally, the combination of molecular engineering with 2D-MXene foresees a promising path forward for the development of Molecular MXetronics, while 3D-printed substrates allow for manufacturing ready-to-use transducers on-demand.

Acknowledgements

Dr. J. M. acknowledges the financial support from the European Union's Horizon 2020 research and innovation programme under the Marie Skłodowska-Curie grant agreement No. 101027867. Prof. M.P. acknowledges the financial support of the Grant Agency of the Czech Republic by the GACR EXPRO 19-26896X project. Authors acknowledge CzechNanoLab Research Infrastructure supported by LM2018110 MEYS CR 2020–2022.

CRedit authorship contribution statement

Dr. J. M. and Dr. M. P.-C. carried out together the conceptualization, investigation and material characterization. Dr. J. M. performed the electrochemical measurements and wrote the original draft. Dr. M. P.-C. synthesized the photo-responsive AZO@Ti₃C₂T_x material and contributed to write the original draft. Prof. M. P. supervised and reviewed the work. All authors have given approval to the final version of the manuscript.

References

- 1 G. E. Moore, *IEEE Solid-State Circuits Soc. Newsl.*, 2009, **11**, 33–35.
- 2 R. E. Fontana and G. M. Decad, *AIP Adv.*, 2018, **8**, 056506.
- 3 N. Margalit, C. Xiang, S. M. Bowers, A. Bjorlin, R. Blum and J. E. Bowers, *Appl. Phys. Lett.*, 2021, **118**, 220501.
- 4 S. Pearton, *Nat. Mater.* 2004 34, 2004, **3**, 203–204.
- 5 M. Schulz, *Nat.* 1999 3996738, 1999, **399**, 729–730.
- 6 K. Kim, J. Y. Choi, T. Kim, S. H. Cho and H. J. Chung, *Nat.* 2011 4797373, 2011, **479**, 338–344.
- 7 N. Fuentes, A. Martín-Lasanta, L. Álvarez De Cienfuegos, M. Ribagorda, A. Parra and J. M. Cuerva, *Nanoscale*, 2011, **3**, 4003–4014.
- 8 F. M. Raymo, *Adv. Mater.*, 2002, **14**, 401–414.

- 9 J. L. Zhang, J. Q. Zhong, J. D. Lin, W. P. Hu, K. Wu, G. Q. Xu, A. T. S. Wee and W. Chen, *Chem. Soc. Rev.*, 2015, **44**, 2998–3022.
- 10 Klaus Schwab, *The Fourth Industrial Revolution*, Ed. Crown Business, New York, 1st Edition, 2016.
- 11 C. Zhai, T. Li, H. Shi and J. Yeo, *J. Mater. Chem. B*, 2020, **8**, 6562–6587.
- 12 B. Daly, T. S. Moody, A. J. M. Huxley, C. Yao, B. Schazmann, A. Alves-Areias, J. F. Malone, H. Q. N. Gunaratne, P. Nockemann and A. P. de Silva, *Nat. Commun.* 2019 101, 2019, **10**, 1–7.
- 13 X. Zhang, L. Chen, K. H. Lim, S. Gonuguntla, K. W. Lim, D. Pranantyo, W. P. Yong, W. J. T. Yam, Z. Low, W. J. Teo, H. P. Nien, Q. W. Loh and S. Soh, *Adv. Mater.*, 2019, **31**, 1804540.
- 14 C. Buten, L. Kortekaas, B. Jan Ravoo, C. Buten, L. Kortekaas and B. J. Ravoo, *Adv. Mater.*, 2020, **32**, 1904957.
- 15 E. Orgiu, N. Crivillers, M. Herder, L. Grubert, M. Pätzl, J. Frisch, E. Pavlica, D. T. Duong, G. Bratina, A. Salleo, N. Koch, S. Hecht and P. Samorì, *Nat. Chem.* 2012 48, 2012, **4**, 675–679.
- 16 K. Szaciłowski, *Chem. Rev.*, 2008, **108**, 3481–3548.
- 17 D. Molinnus, A. Poghossian, M. Keusgen, E. Katz and M. J. Schöning, *Electroanalysis*, 2017, **29**, 1840–1849.
- 18 M. Gobbi, S. Bonacchi, J. X. Lian, A. Vercouter, S. Bertolazzi, B. Zyska, M. Timpel, R. Tatti, Y. Olivier, S. Hecht, M. V. Nardi, D. Beljonne, E. Orgiu and P. Samorì, *Nat. Commun.* 2018 91, 2018, **9**, 1–9.
- 19 J. M. Macleod and F. Rosei, *Small*, 2014, **10**, 1038–1049.
- 20 J. Muñoz, E. Redondo and M. Pumera, *ACS Appl. Mater. Interfaces*, 2021, **13**, 12649–12655.

- 21 M. Hu, H. Zhang, T. Hu, B. Fan, X. Wang and Z. Li, *Chem. Soc. Rev.*, 2020, **49**, 6666–6693.
- 22 F. Shahzad, S. A. Zaidi and R. A. Naqvi, *Crit. Rev. Anal. Chem.*, 2022, **52**, 848–864.
- 23 Xing Li, Yang Bai, Xian Shi, Na Su, Gongzhe Nie, Rumeng Zhang, Hongbo Nie and Liqun Ye, *Mater. Adv.*, 2021, **2**, 1570–1594.
- 24 K. Gong, K. Zhou, X. Qian, C. Shi and B. Yu, *Compos. Part B Eng.*, 2021, **217**, 108867.
- 25 C. E. Shuck, A. Sarycheva, M. Anayee, A. Levitt, Y. Zhu, S. Uzun, V. Balitskiy, V. Zahorodna, O. Gogotsi and Y. Gogotsi, *Adv. Eng. Mater.*, 2020, **22**, 1901241.
- 26 D. Xiong, X. Li, Z. Bai, S. Lu, D. Xiong, X. Li, Z. Bai and S. Lu, *Small*, 2018, **14**, 1703419.
- 27 H. Kim and H. N. Alshareef, *ACS Mater. Lett.*, 2019, **2**, 55–70.
- 28 H. Kim, Z. Wang and H. N. Alshareef, *Nano Energy*, 2019, **60**, 179–197.
- 29 V. H. Nguyen, R. Tabassian, S. Oh, S. Nam, M. Mahato, P. Thangasamy, A. Rajabi-Abhari, W. J. Hwang, A. K. Taseer and I. K. Oh, *Adv. Funct. Mater.*, 2020, **30**, 1909504.
- 30 T. Zhou, C. Wu, Y. Wang, A. P. Tomsia, M. Li, E. Saiz, S. Fang, R. H. Baughman, L. Jiang and Q. Cheng, *Nat. Commun. 2020 111*, 2020, **11**, 1–11.
- 31 P. Mayorga-Burrezo, J. Muñoz, D. Zaoralová, M. Otyepka and M. Pumera, *ACS Nano*, 2021, **15**, 10067–10075.
- 32 W. Y. Chen, S. N. Lai, C. C. Yen, X. Jiang, D. Peroulis and L. A. Stanciu, *ACS Nano*, 2020, **14**, 11490–11501.
- 33 W. Yang, B. Huang, L. Li, K. Zhang, Y. Li, J. Huang, X. Tang, T. Hu, K. Yuan and Y. Chen, *Small Methods*, 2020, **4**, 2000434.

- 34 J. T. Lee, B. C. Wyatt, J. Gregory A. Davis, A. N. Masterson, A. L. Pagan, A. Shah, B. Anasori and R. Sardar, *ACS Nano*, 2021, **10**, acsnano.1c06670.
- 35 R. D. Mukhopadhyay, V. K. Praveen and A. Ajayaghosh, *Mater. Horizons*, 2014, **1**, 572–576.
- 36 H.-B. Cheng, S. Zhang, J. Qi, X.-J. Liang, J. Yoon, -B H Cheng, S. Zhang, J. Qi, -J X Liang and J. Yoon, *Adv. Mater.*, 2021, **33**, 2007290.
- 37 W. Feng, W. Luo and Y. Feng, *Nanoscale*, 2012, **4**, 6118–6134.
- 38 S. Chen, Y. Xiang, C. Peng, J. Jiang, W. Xu and R. Wu, *J. Power Sources*, 2019, **414**, 192–200.
- 39 J. Muñoz, E. Redondo, M. Pumera, J. Muñoz, E. Redondo and M. Pumera, *Adv. Funct. Mater.*, 2021, **31**, 2010608.
- 40 J. Muñoz and M. Pumera, *Chem. Eng. J.*, 2021, **425**, 131433.
- 41 J. Muñoz, E. Redondo and M. Pumera, *Appl. Mater. Today*, 2022, **28**, 101519.
- 42 H. W. Tan, Y. Y. C. Choong, C. N. Kuo, H. Y. Low and C. K. Chua, *Prog. Mater. Sci.*, 2022, **127**, 100945.
- 43 M. P. Browne, F. Novotný, Z. Sofer and M. Pumera, *ACS Appl. Mater. Interfaces*, 2018, **10**, 40294–40301.
- 44 J. Muñoz, E. Redondo, M. Pumera, J. Muñoz, E. Redondo and M. Pumera, *Small*, 2021, **17**, 2103189.
- 45 M. Ding, H. Xu, W. Chen, G. Yang, Q. Kong, D. Ng, T. Lin and Z. Xie, *J. Memb. Sci.*, 2020, **600**, 117871.
- 46 K. Qian, S. Li, J. Fang, Y. Yang, S. Cao, M. Miao and X. Feng, *J. Mater. Sci. Technol.*, 2022, **127**, 71–77.
- 47 W. Xu, S. Hu, Y. Zhao, W. Zhai, Y. Chen, G. Zheng, K. Dai, C. Liu and C. Shen, *Nano Energy*, 2021, **90**, 106606.

- 48 S. Sun, S. Liang, W. C. Xu, G. Xu and S. Wu, *Polym. Chem.*, 2019, **10**, 4389–4401.
- 49 M. Jiang, Y. Yin, W. Cai, J. Zhang, L. Fan, Y. Yi, Y. Dai, T. Zhou and J. Liu, *J. Appl. Polym. Sci.*, 2021, **138**, 50731.
- 50 S. N. Yogitha, B. Kumar, Raghavendra, Imranpasha and S. K. Gupta, *Mater. Sci. Eng. B*, 2021, **267**, 115094.
- 51 V. Ferri, M. Elbing, G. Pace, M. D. Dickey, M. Zharnikov, P. Samorì, M. Mayor, M. Anita Rampi, G. Pace, P. Samorì, M. Mayor, V. Ferri, M. A. Rampi, M. Elbing, M. D. Dickey and M. Zharnikov, *Angew. Chemie Int. Ed.*, 2008, **47**, 3407–3409.
- 52 F. Cicogna, I. Domenichelli, S. Coiai, F. Bellina, M. Lessi, R. Spiniello and E. Passaglia, *Data Br.*, 2016, **6**, 562–570.
- 53 S. Schimka, Y. D. Gordievskaya, N. Lomadze, M. Lehmann, R. Von Klitzing, A. M. Rumyantsev, E. Y. Kramarenko and S. Santer, *J. Chem. Phys.*, 2017, **147**, 031101.
- 54 J. Muñoz, A. González-Campo, M. Riba-Moliner, M. Baeza and M. Mas-Torrent, *Biosens. Bioelectron.*, 2018, **105**, 95–102.